Studies on Adsorption and Dissociation of Methane and Carbon Dioxide on Nickel Catalyst

*Ling Qian, Zi-Feng Yan**

Division of Fuel Chemistry
State Key Laboratory for Heavy Oil Processing
University of Petroleum
Dongying, China 257061

Introduction

During the past decades, the process of carbon dioxide reforming with methane has received attention, and efforts have focused on development of catalysts which show high activity towards synthesis gas formation, and are also resistant to carbon formation, thus displaying stable long-term operation[1]. One reason for this renewed interest is of environmental considerations since the reaction consumes carbon dioxide and methane, which are the serious well-known greenhouse gases. Another factor leading to the increased interest in the process is that this reaction offers a suitable H_2/CO ratio needed in F-T synthesis. The key to this process is to develop the optimum catalysts. Numerous materials have been tested as potential catalysts for carbon dioxide reforming with methane, while supported noble metal catalysts as well as Ni-based catalysts have been found to exhibit promising catalytic performance[2-3]. However, the major obstacle encountered in this process is rapid catalyst deactivation by carbon deposition on nickel catalyst surface.

Carbon deposition over catalysts is the fatal problem for carbon dioxide reforming with methane. Although some noble metals show high activity and selectivity for carbon-free operation, high cost and limited availability of noble metals prevent the commercial use of this reaction. It is, therefore, more practical to develop an improved nickel-based catalyst which exhibits stable operation for a long period of time.

Carbon dioxide reforming with methane are particularly important reactions took place on a metal surface. Despite their potential usefulness in energy industry and environment optimization, the nature of the active carbonaceous species produced by the dissociative adsorption of methane and/or carbon dioxide and the detailed mechanism of the reforming reactions are not yet known. It is rather important to clarify the stability, reactivity, selectivity and other properties of the carbonaceous species adsorbed on a metal surface.

Experimental

Catalyst Preparation. The supported nickel catalysts were prepared by a conventionally incipient wetness impregnation method, with aqueous solutions of nitrates as promoter and metal precursors[4]

Catalyst Characterization. The catalyst sample (100mg) was firstly pretreated in an O_2 flow of 20ml/min at 973K for 30min, then the O_2 flow was switched to a H_2 flow of 30ml/min and reduced for 1hr. After the sample was cooled to room temperature in H_2 flow, a 30ml/min He flow was introduced to purge the sample for 30min.

TPR, TPD, TPSR and pulse reaction experiments were carried out in an apparatus, which consisted of a flow switching system, a heated reactor, and an analysis system (**Fig. 1**).

Correspondence should be addressed. E-mail: zfyancat@hdpu.edu.cn zfyan@hdpu.edu.cn

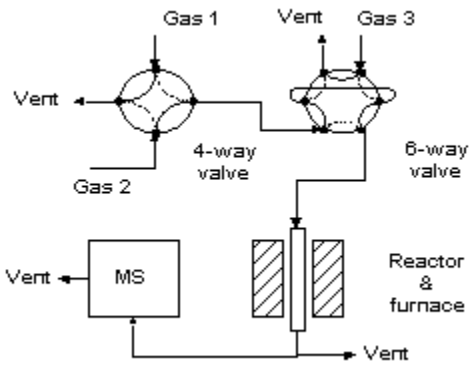

Figure 1. Schematic of the transient response kinetic analysis system

TPSR experiments were also performed in the quartz-fixed-bed micro-reactor. CH_4 was continually pulsed into the catalyst at certain temperature and then the reactor was quickly cooled to room temperature. Subsequently, a 30ml/min flow of H_2/He (1:2) or CO_2/He (1:10) was introduced to flush the reactor continuously to take away the mixture of gases and physically adsorbed. After that treatment, the surface intermediate species produced in the reforming process were well characterized by TPSR in the mixed gas flow. The desorbed species from the metal surface along with the temperature-programmed process were simultaneously detected by the *on-line* DYCOR quadrupole mass spectrometer.

TPD experiments were conducted at a constant heating rate (23K/min), using ultra high purity He as carrier gas, at a flow rate of 30ml/min. When the required adsorption temperature reached, the flow was switched to CO or CH_4 flow. The tested gas adsorbed on the sample for 30 min. Then the flow was switched again to flush the reactor after cooling to room temperature in the adsorption gas flow. Next temperature programming was initiated and the analysis of the desorbed gases was performed with an *on-line* quadrupole mass spectrometer (DYCOR Quadrupole, Ametek Instrument). In the TPD process, the helium gas was dried with $Mg(ClO_4)_2$ and deoxygenated with 402 deoxygenating reagent. The residual oxygen in carrier gas that flowed over the catalyst was removed by cold trap of liquid nitrogen before flowing into the reactor. Leak tests on the reaction system were also strictly performed to exclude the possibility of the oxidation of surface carbon.

XPS for nickel samples was conducted on a VG ESCALAB 210 X-ray photoelectron spectrometer with Mg Kα radiation and a base pressure of 10^{-8}Pa. The specially designed pretreatment cell made sure that the transfer of the XPS sample was not exposed to air before XPS experiments. The Si_{2p} level, with a binding energy of 102.7eV, was used to correct the charge effect as the reference line. The Fisons Eclipse Data System was used to perform the data acquisition and analysis.

The pulse reaction experiments were conducted in the quartz fixed-bed reactor following the catalysts pretreatment. Methane was pulsed continually on the pretreated catalysts using high purity helium as carrier gas at 973K. Subsequently, a 20ml/min flow of H_2/He (1:2) or CO_2/He (1:10) mixture was introduced to flush the reactor continuously to take away the gaseous and physically adsorbed mixture. Then TPSR was initiated in the flow of H_2/He (1:2) or CO_2/He (1:10) at a heating rate of 23K/min. When the temperature was increased to 973K, the carrier gas was switched again, then 0.39ml of H_2, CO_2, or O_2 were continually pulsed respectively into the micro-reactor under high temperature. The desorbed products from the metal surface were simultaneously detected by the *on-line* DYCOR quadrupole mass spectrometer.

Results and Discussion

Methane decomposition on transition metal surface is a thermally assisted catalytic activated process. The reactive sticking of alkanes on nickel single crystal surfaces is strongly dependent on the surface structure. For example, methane reactivity is seen to increase in the order of Ni (111) < Ni (110) < Ni (100) with prolonged exposure to methane[5]. Initial reaction rates for Ni (110) and Ni (100) surfaces are rather similar, and are 7~10 times greater than the initial rate for the Ni (111) surface at 450K. In this study, several questions are addressed. Firstly, how do carbonaceous fragments, in particular the simplest fragment-$CH_{x(ad)}$ species, bond to metal surfaces with more complex structure than that to single crystal surfaces? Secondly, low-index nickel single crystal surface should be effective toward the decomposition of methane, but can alumina-supported nickel catalyst surface be effective in the decomposition of methane? What is the mechanism of thermal decomposition of methane on alumina-supported nickel catalysts? TPSR, TPD, XPS techniques are used to identify surface-bound species and gas-phase products of decomposition of methane adsorbed on alumina-supported nickel catalysts.

For the reaction of CO_2 reforming with methane, the most probable slow steps are methane activation to $CH_{x(ad)}$ (x = 0 ~ 3) species, and the reaction between $CH_{x(ad)}$ species and the oxidant, either in the form of oxygen adatoms originated from CO_2 dissociation or CO_2 itself. Experiments have confirmed that methane promotes the dissociation of carbon dioxide on the catalysts. The promotion of carbon dioxide is attributed to the effect of hydrogen formed in the decomposition of methane. It seems that the key to elucidation the nature of the CO_2 reforming with methane over Ni/γ-Al_2O_3 catalyst is to reveal mechanistic scheme of activation and dissociation of methane.

A great effort was made to detect adsorbed carbonaceous $CH_{x(ad)}$ fragments formed in the decomposition of methane by means of sensitive *in-situ* FT-IR spectroscopy. However, no adsorption bands attributable to any vibration modes of carbonaceous $CH_{x(ad)}$ species were identified either by *in-situ* measurements or after a sudden cooling of the sample in a continuous methane flow at 700K. This means that carbonaceous $CH_{x(ad)}$ species react or decompose too quickly at high temperature, or their surface concentrations are below the detection limit.

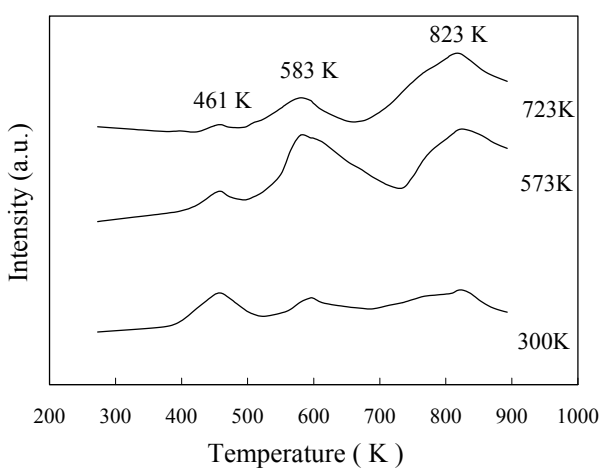

Figure 2. TPSR spectra of CH_4 in H_2 flow on fresh 8wt% Ni/Al_2O_3 at different adsorption temperatures

However, the presence of surface carbonaceous $CH_{x(ad)}$ species was well manifested by its reaction with hydrogen. After flushing the reactor with H_2/He (1:2) flow (following methane decomposition at a certain temperature), the hydrogenation of the surface carbonaceous $CH_{x(ad)}$ species was investigated by TPSR technique. **Figure 2** showed that the decomposition of methane could result in the formation of at least three kinds of surface carbon species on supported nickel catalyst. Generally, the carbon deposition is comprised of various forms of carbons, which are different in terms of reactivity. The distribution and features of these carbonaceous species depend sensitively on the nature of transition metals and the conditions of methane adsorption. These carbonaceous species can be described as: completely dehydrogenated carbidic C_α type, partially dehydrogenated CH_x ($1 \le x \le 3$) species, namely C_β type, and carbidic clusters C_γ type formed by the agglomeration and conversion of C_α and C_β species under certain conditions. A fraction of the surface carbon species, which might be assigned to carbidic C_α (~461K), was mainly hydrogenated to methane even below 500K. It showed that carbidic C_α species is rather active and thermally unstable on nickel surface. The carbidic C_α species was suggested to be responsible for CO formation[6]. The significant amount of surface carbon species was hydrogenated to methane below 600K and was assigned to partially dehydrogenated C_β (~583K) species. The majority of the surface carbon was hydrogenated above 800K and was attributed to carbidic clusters C_γ (~823K) [6].

It also indicated that the formation of three kinds of surface carbon species with different structures and properties largely depend on the exposure temperature and duration to methane. When the nickel catalyst was exposed to methane above 723K, the carbidic C_α species was not detected, and a significant amount of C_β was transformed into the carbidic clusters C_γ. It showed that the carbidic clusters C_γ species might be the precursor of the surface carbon deposition, which may be produced by the interactions between C_α and C_β species and between C_α and C_β themselves.

Figure 3 showed CO_2 TPD on fresh 8wt% Ni/Al_2O_3 catalyst after pretreatment. CO_2 was adsorbed on the catalyst at room temperature (300K). A broad CO_2 desorption peak appeared at 420K on the CO_2 TPD profiles and CO desorption was not detected. This exhibited that CO_2 weakly adsorbed on the catalyst and only a kind of adsorption state of CO_2 formed. From the point of thermodynamic view, dissociated adsorption of CO_2 is impossible on the reduced nickel catalyst. Hereby, it was reasonable that no CO_2 dissociation was observed from TPD profiles.

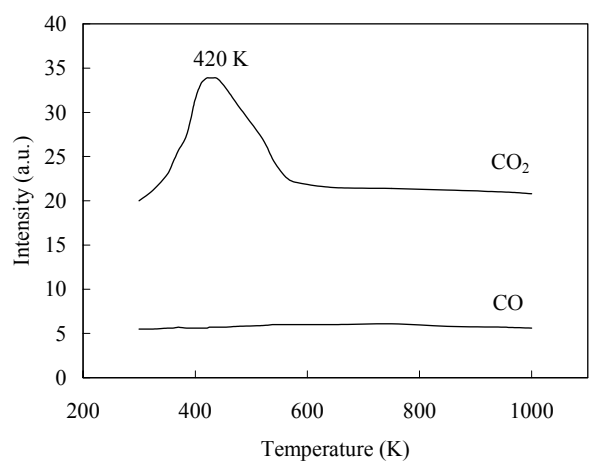

Figure 3. CO_2 TPD over fresh 8wt% Ni/Al_2O_3 catalyst

The CO TPD profiles over the fresh Ni/Al_2O_3 catalyst were

obtained following CO adsorption at 300K (**Figure 4**). The response of CO_2 formation was recorded to monitor the occurrence of CO disproportionation during the process of temperature programming. It was observed that two apparent CO_2 desorption peaks appeared at 410K and 570K, but the intensity of CO remained almost unchanged. The CO_2 desorption peak at 410 K was similar to the CO_2 peak on the CO_2 TPD profiles, which desorbed at 420K. It indicated that CO disproportionation reaction occurred at room temperature and weakly adsorbed CO_2 was formed. The CO_2 desorption at 570K may be derived from disproportionation of strongly adsorbed CO on the catalyst.

As shown in **Figure 5**, TPD spectra of methane on fresh Ni/Al_2O_3 catalyst exhibited that three corespondent peaks of CO_2 were observed. It means that methane decomposition on transition metals truly takes place and the reactivity of the surface carbon species depends sensitively on the varieties of the reactions.

For TPSR spectra in the flow of hydrogen, desorbed product is mainly methane (Figure 2). But for TPD spectra in the flow of helium, desorbed species were mainly CO_2 and some CO, which means that the TPD process was actually a process of temperature-programmed oxidation (TPO), in which the surface carbon was oxidized to form CO and CO_2. The surface oxygen species, which resulted in the oxidation of surface carbon, might be the residual or remaining surface bonded oxygen (M-O) on transition metals. The oxygen atoms in subsurface and bulk phase of the metal cannot migrate to the surface below 1000K[7].

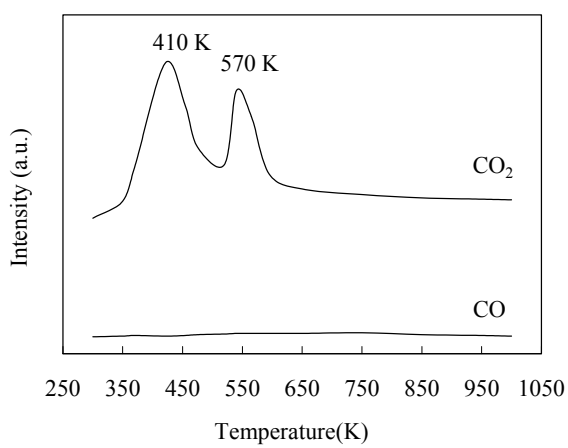

Figure 4. CO TPD over fresh 8wt% Ni/Al_2O_3 catalyst.

Furthermore, XPS results showed that the crystalline oxygen of alumina support does not interact with the surface carbon at moderate temperature (< 850K). Thus, the CO and CO_2 produced during TPD process might originate from the partially reduced oxygen bonded to metal. This kind of bonded oxygen is rather difficult to be reduced under the pretreatment conditions and cannot migrate from one site to another. It also means that the residual NiO_x species dispersed on the surface of supported nickel catalyst were stepwise reduced during the reaction.

During the TPD process, the surface carbon produced by the decomposition of methane might migrate to the sites of bonded oxygen and interact with them to form carbon oxides. It means that peak temperature gaps (ΔT) of correspondent surface carbon species between TPD and TPSR might be the parameters of characterizing the mobility of the different surface carbon (Figure 2 and 5). An examination of the peak temperature gap indicated that the mobility of different surface carbon species on nickel catalyst is consistent with the order of $C_\gamma > C_\alpha > C_\beta$, with the ΔT value of 0, 5, and 34K, respectively. This indicated that the carbonaceous species formed by the decomposition of methane are mobile enough and interact with partial metal oxide to form CO_2. In the meantime, from Figure 5 another conclusion can be drawn that C_α and C_β species could be transformed into C_γ species and the transformation could be accelerated with the increasing adsorption temperature, similar to those exhibited in TPSR studies (**Figure 2**).

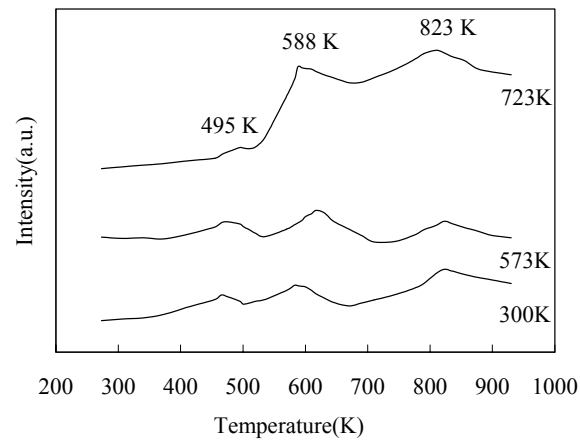

Figure 5. TPD spectra of CH_4 in He flow on fresh 8wt%Ni/Al_2O_3 catalyst at different adsorption temperatures.

The TPD profiles of used Ni/Al_2O_3 catalyst after 4hrs of reforming reaction were shown in **Figure 6**. The response of CO_2 formation was recorded to monitor the occurrence of CO disproportionation during the process of temperature programming. Compared with CO-TPD profiles over the fresh Ni/Al_2O_3 catalyst, on which two respective CO_2 desorption peaks appeared, the TPD profiles on used catalyst were different. An additional intense CO_2 peak at ca. 910K was observed on used catalyst. The CO desorption was also increased with increasing temperature from at ca. 810K.

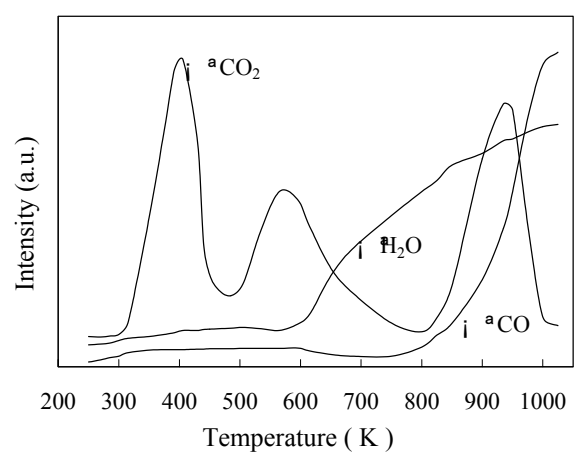

Figure 6. TPD profiles over used 8wt% Ni/Al_2O_3 catalyst after 4hrs of reforming reaction.

The two CO_2 desorption peaks appeared on both CO-TPD profiles over the fresh and used catalysts at ca. 410K and 570K. They seemed to correspond to the desorbed CO_2 in the form of weak chemisorption on different sites on both catalysts. It was interesting to note that a large quantity of CO and CO_2 desorbed at approximately the same temperature from at ca. 800K, but the

increase of CO obviously lagged behind. This could be manifested by the mobility of the surface carbon species and the reactivity of the oxygen species on the nickel catalyst. The mobile surface carbon species can attack the neighboring oxygen adatoms or surface oxygen species to form CO_2. It was also possible that the CO_2 desorbed from the catalyst re-adsorbed and then reacted with surface carbonaceous species to produce CO. The obvious hysteresis effect of CO peak with respect to CO_2 indicated that CO might be the secondary product rather than primary one.

The XPS experiments and Ar^+ etching techniques could give more supporting information. The binding energy data of the catalyst calcined in air at 973K, reduced in H_2 at 973K and exposed to methane followed by reduction were submitted by XPS experiments. The results showed that surface nickel exists in oxidative state (B.E. 856.00eV) for calcined sample, partially oxidative state (B.E. 853.64eV) for reduced sample in H_2 and metallic state (B.E. 852.90eV) for methane exposed sample (Figure 7). The binding energy of metal Ni is 852.30eV, so it is derived that the catalyst exposed to methane following reduction exists essentially in metallic state. This is also consistent with the CH_4 TPD results above (Figure 5). That is to say, the residual NiO_x species dispersed on the surface of supported nickel catalyst can be stepwise reduced during the reaction.

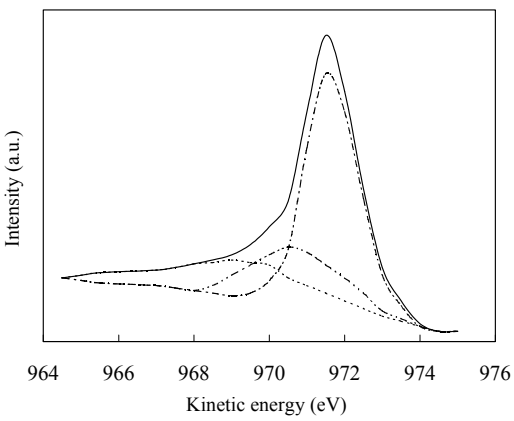

Figure 7. Deconvoluted XPS of C(1s) of 673K-adsorbed CH_4 at 300K.

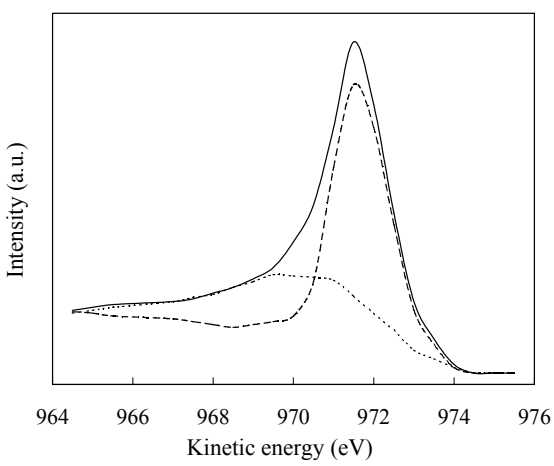

Figure 8. Deconvoluted XPS of C(1s) of 673K-adsorbed CH_4 after sputtered by Ar^+ ions of 1.36×10^{-4}Pa at 300K and 5kV for 5min.

Figure 7 showed that methane decomposition on supported nickel catalyst can result in three different types of surface carbon, similar to the TPSR results, whose binding energy are 282.00, 282.90 and 284.70eV, respectively. The deconvoluted XPS spectra of C(1s) of 673K-adsorbed CH_4 after sputtered by Ar^+ at 300K were shown in **Figure 8**. Comparison of deconvoluted XPS spectra before and after Ar^+ etching exhibited that C_α (B.E. 282.00eV) and C_β (B.E. 282.90eV) species are thermally unstable and can be transformed into C_γ species (B.E. 284.70eV) under the experimental conditions.

As shown in **Figure 9**, CO_2 TPSR was firstly performed in the mixed gas of CO_2/He (1:10) following CH_4 pulses over reduced Ni/Al_2O_3 catalyst, then the H_2 or O_2 pulse was introduced into the reactor (**Figure 10**). In the same way, H_2 TPSR was performed in the mixed gas of H_2/He (1:2) flow following CH_4 pulses over reduced Ni/Al_2O_3 catalyst, then the CO_2 or O_2 pulse was introduced into the reactor (**Figure 11**).

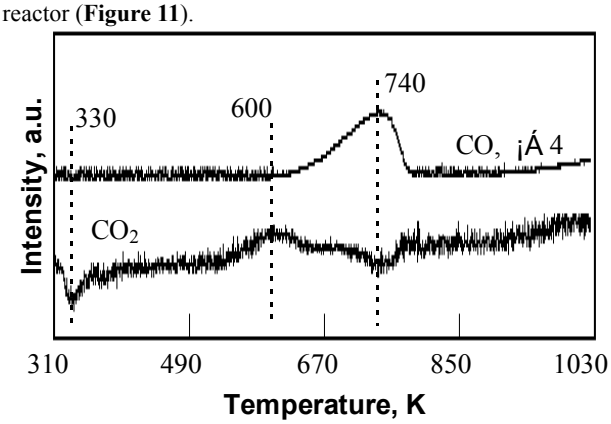

Figure 9. TPSR in CO_2/He (1:10) stream following CH_4 pulses at 973K over reduced Ni/Al_2O_3 catalyst.

A fraction of CO_2 adsorbed on the catalyst at about 300K and desorbed from 600K in the CO_2/He flow. The equilibrium between the surfaced adsorbed CO_2 and gaseous CO_2 was responsible for the high CO_2 desorption temperature than that in He flow (420K). The formation and desorption of CO can be observed while surfaced CO_2 began to desorb greatly. The consumption of CO_2 and formation of CO reached the maximum at increased temperature of 740K. CO_2 TPSR on the Ni catalyst may give a deduction of the reaction pathway of CO_2: firstly adsorbed on the surface of the catalyst, then reacted with neighboring surface carbonaceous species to form CO. This was similar to the inference from the TPD experiment of the used catalyst as **Figure 5** showed.

The formation of CH_4 was not detected in the H_2 pulse reaction following CO_2 TPSR at 973K. It showed that the surface carbonaceous species, which can react with CO_2 feed, had used up. The formation of CO was not detected in the CO_2 pulse reaction following H_2 TPSR at 973 K, either. It showed that the surface carbonaceous species which can react with H_2 had used up. This type of surface carbonaceous species was active and can react with not only CO_2 but also with H_2. At the same time, other inertial carbonaceous species may exist on the surface of the catalyst. The O_2 pulse reaction was continually carried out following the H_2 or CO_2 pulse reaction in order to verify the existence of other carbonaceous species. The appearance of CO_2 pulses was good evidence for the existence of the other carbonaceous species, which was difficult to react with H_2 or CO_2. The catalyst deactivation may result from the deposited carbon species which only reacts with O_2 even at very high temperature.

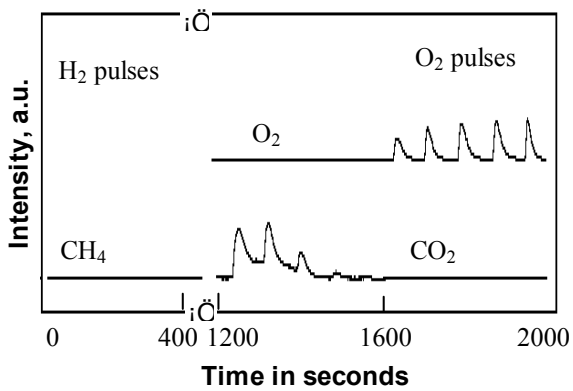

Figure 10. H_2 and O_2 pulses patterns at 973K following CO_2 TPSR over Ni/Al_2O_3 catalyst.

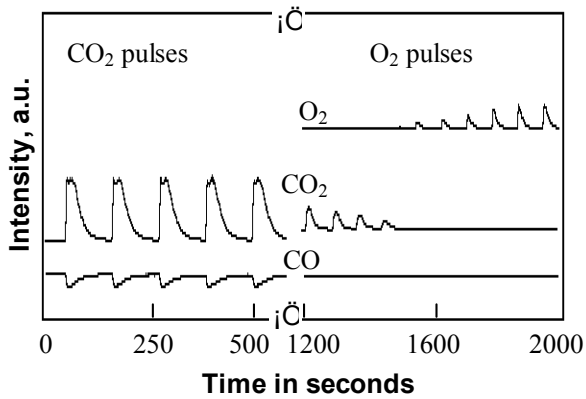

Figure 11. CO_2 and O_2 pulse patterns at 973K after H_2 TPSR over Ni/Al_2O_3 catalyst.

Figure 2 became conscious of the emergence of at least three kinds surface carbonaceous species produced by the decomposition of methane at lower temperature. When the catalyst was exposed to methane at 973K, the carbidic C_α species was completely converted into C_β or C_γ species. The partially dehydrogenated C_β species can react with H_2 or CO_2 to form CH_4 or CO, but the less active carbidic clusters C_γ species can not react with H_2 or CO_2, but react with O_2 at high temperature. The H_2 and CO_2 TPSR and pulse reaction provide the mutual verification of the existence and property of the surface carbonaceous species.

Based on all the above studies, the possible reaction processes of carbon dioxide reforming with methane can be inferred as follows: methane is firstly decomposed into hydrogen and different surface carbon species, then the absorbed CO_2 reacts with surface carbons to form CO. The pattern of activation and reaction of methane with carbon dioxide on the supported nickel catalysts is shown as **Figure 12**.

Conclusions

TPSR and TPD showed that the decomposition of methane results in the formation of at least three kinds of surface carbon species on supported nickel catalyst and that the distribution and features of these carbonaceous species depend sensitively on the nature of transition metals and the conditions of methane adsorption.

Carbidic C_α, carbonaceous C_β and carbidic clusters C_γ surface carbon species formed by decomposition of methane showed different surface mobility, thermal stability and reactivity. C_α and C_β species on the nickel surface are thermally unstable and can be rapidly converted into C_γ species upon the increasing temperature. The carbidic carbon is a very active and important intermediate in the carbon dioxide reforming with methane and the carbidic clusters C_γ species might be the precursor of the surface carbon deposition.

CO_2 TPD exhibited that CO_2 weakly adsorbs on the catalyst and only a kind of adsorption state of CO_2 formed. CO TPD indicated two kinds of adsorption states of CO exist on the catalyst and desorbed in the form of CO_2 at different temperatures by the CO disproportionation reaction.

The CH_4 TPD process actually undergoes a TPO process involving the surface residual oxygen species on reduced nickel catalyst. CO and CO_2 produced during TPD process might originate from the partially reduced residual oxygen bonded to metal. It can be used to evaluate the mobility of the surface carbon species.

The partially dehydrogenated C_β species can react with H_2 or CO_2 to form CH_4 or CO, but the less active carbidic clusters C_γ species can not react with H_2 or CO_2, but react with O_2 at high temperature. The catalyst deactivation may result from the deposited carbon species which only reacts with O_2 even at very high temperature.

The possible interaction mechanism of carbon dioxide reforming with methane is that methane is firstly decomposed into hydrogen and different surface carbon species, then the absorbed CO_2 reacts with surface carbons to form CO.

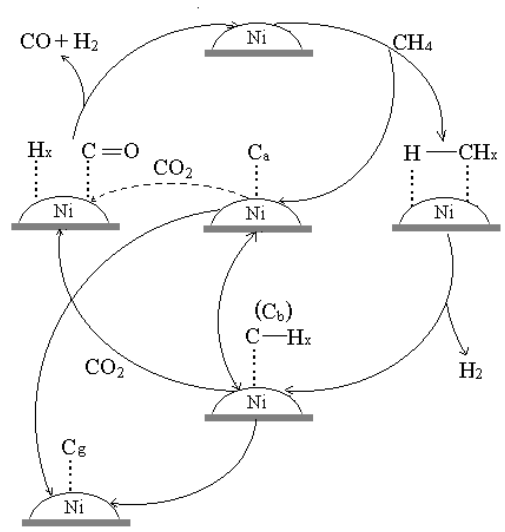

Figure 12. Patterns of activation and reaction of CH_4 with CO_2 on the nickel catalyst (C_a represents carbidic species – C_α, C_b represents carbonaceous species – C_β, C_g represents carbidic clusters species – C_γ. The dotted line represents less possible pathway.)

References

(1) Fischer, V. F.; Tropsch, H. *Brennst. Chem.,* **1928**, *3*(9), 39.
(2) Ding, R.-G.; Yan, Z.-F.; Qian, L. *Natural Gas Chemical Industry (Tianranqi Huagong)*, **1999**, *24*, 50.
(3) Rostrup-Nielsen, J. R.; Hansen, J. H. B. *J. Catal.,* **1993**, *144*, 38.
(4) Yan, Z.-F.; Ding, R.-G.; Song, L.-H.; Qian, L. *Energy & Fuels*, 1998, *12*, 1114.
(5) Beebe, T.P.; Goodman, D.W.; Kay, B.D.; Yates, J.T. *J. Chem. Phys*., **1988**, *92*, 5213.
(6) Zhang, Z.; Verykois, X. E. *Catal. Today,* **1994,** *21*, 589.
(7) Yan, Z.-F.; Xue, J.-Z.; Shen, S.-K. *J. Natural Gas Chem*., **1996**, *5*, 51.